ISSN 0020-1685, Inorganic Materials, 2010, Vol. 46, No. 1, pp. 51–54. © Pleiades Publishing, Ltd., 2010.

A Facile Template-Free Preparation of Porous Manganese Oxides by Thermal Decomposition Method[1]

Xianzhong Zhang[a], Linhai Yue[a], Dalai Jin[b], and Yifan Zheng[c]

[a]*Chemistry Department, Zhejiang University, Hangzhou 310027, People's, Republic of China*
[b]*Center of Materials Engineering, Zhejiang Sci-Tech University, Xiasha University Town, Hangzhou 310018, People's Republic of China*
[c]*College of Chemical Engineering and Materials Science, Zhejiang University of Technology, Hangzhou 310014, People's Republic of China*
e-mail: zjchem_yue@126.com

Received January 12, 2009

Abstract—Porous Manganese oxides with large surface area were prepared by a facile template-free method. Highly crystallized $MnCO_3$ precursors with micron size in high dispersivity were prepared in water first. Thermal treatment was carried out with the obtained composite at different temperatures to produce porous manganese oxides. Thermogravimetry and differential thermal analysis (TG-DTA), X-ray powder diffraction (XRD), Scanning electron microscopy (SEM) and N_2 adsorption-desorption measurements were applied to characterize the porous manganese oxides. Amorphous MnO_2 obtained at 400°C shows a mesoporous structure and has a large specific surface area of 135.1 m^2/g. Well crystallized α-Mn_2O_3 crystal with surface area of 18.51 m^2/g macroporous framework was obtained at 600°C.

DOI: 10.1134/S0020168510010127

INTRODUCTION

Porous oxides of transition metals hold many advantages over aluminosilicate materials in areas of electromagnetics, photoelectronics and catalysis because transition metal atoms can exist in various oxidation states [1]. In particular, manganese oxides have attracted considerable attentions due to their wide applications as catalysts [2], adsorbents [3], magnetic materials [4], sensors [5] and supercapacitor electrode materials [6]. Since manganese oxides have various advantages such as low cost, eco-friendly property and fascinating application potentials, many efforts have been devoted to the synthesis of porous manganese oxides around the world.

Most of the methods applied in synthesizing the porous manganese oxides were reported to use of template technique [7] in the past decade. Xu and his coworkers synthesized amorphous MnO_2 via reduction route using supramolecular as template and the product exhibited excellent electrochemical is property [8]. The amorphous mesoporous MnO_2 was reported to be prepared by sonochemical method using surface modified SBA-15 as hard template. It showed a specific surface area of 91 m^2/g [9]. Macroporous Mn_2O_3 was synthesized by Andreas Stein Group using polystyrene spheres as template, and the product showed a BET surface area of 20 m^2/g [10]. Although templates facilitated the formation of the pore structure, expensive template agents were required and the purity of the products was uncertain as removing the precursors. Furthermore, the use of soft template caused low crystallinity. Its low heat-resistivity above 400°C tended to cause pore structure collapse at high temperature. The strategy without the assistance of templates seems more desirable in the preparation of porous manganese oxides.

In this paper, a facile but novel template-free approach was reported for preparing porous manganese oxides. Micron sized $MnCO_3$ crystal was synthesized by a simple precipitation reaction. Porous manganese oxides were then successfully prepared by direct thermal decomposition of precursor in static air without any additives. Amorphous MnO_2 with mesoporous structure and crystallized pure α-Mn_2O_3 with macroporous structure were obtained. Similar method has been applied in the formation of microporous Mn_2O_3 by thermal decomposition of monoclinic manganese oxalate in our previous work [11].

EXPERIMENTAL

Synthesis. All the chemical reagents are of analytical grade and purchased from Shanghai Chemical Reagent Company which were used without further purification. 0.2 mol/L Na_2CO_3 solution was first prepared, then 0.2 mol/L $MnCl_2$ solution was dripped down in to the Na_2CO_3 solution while strong magnetic stirring was applied at 30°C. Keep stirring for 30 minutes after the reaction. The precipitation was aged

---

[1] The article is published in the original.

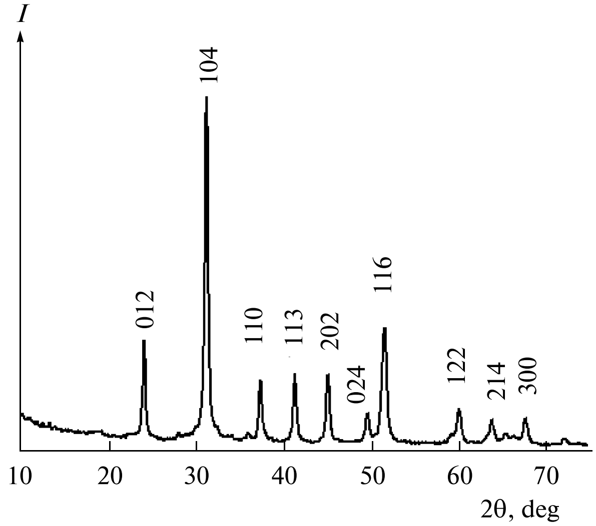

Fig. 1. XRD pattern of the precursor $MnCO_3$.

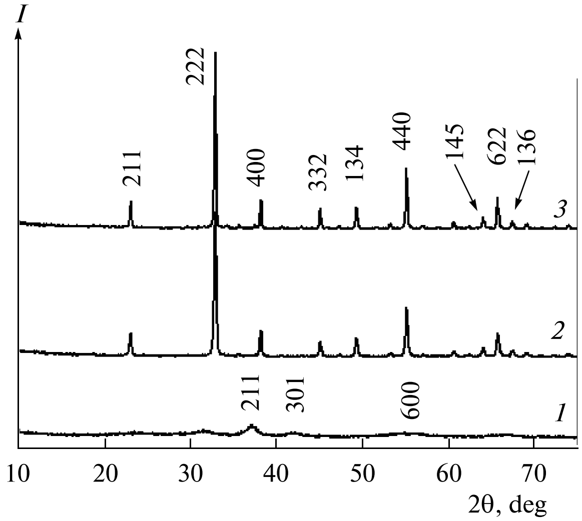

Fig. 3. XRD patterns of the calcined samples: CT400 (*1*), CT600 (*2*), CT800 (*3*).

statically for 4 h and then filtered, washed with distilled water for several times and dried in an oven at 90°C for 12 h.

Thermal treatment was carried out with the obtained precursor in a muffle furnace at temperatures of 400, 600, 800°C for 2 h, the heating rate during calcinations was controlled to be 10°C/min. The final products were labeled as CT400, CT600, CT800.

Characterization. X-ray diffraction (**XRD**) of the powder sample was performed by a Philips X Pert MPD diffractometer using CuK_α radiation (λ = 0.15405 nm). Scan rate of 4°/min and step size of 0.04° were applied to record the pattern in the 2θ range 10°–75°. The operation voltage and current were 40 kV and 45 mA respectively. SEM images of the samples were recorded on a Hitachi S-4700 model scanning electron microscopy. TG-DTA curves were determined by a WCT-1 apparatus at a heating rate of 10°C/min in atmosphere. N_2 adsorption-desorption isotherms were measured in a NOVA 1000e instrument at 77.36 K. The resulting isotherms were analyzed by the BET method.

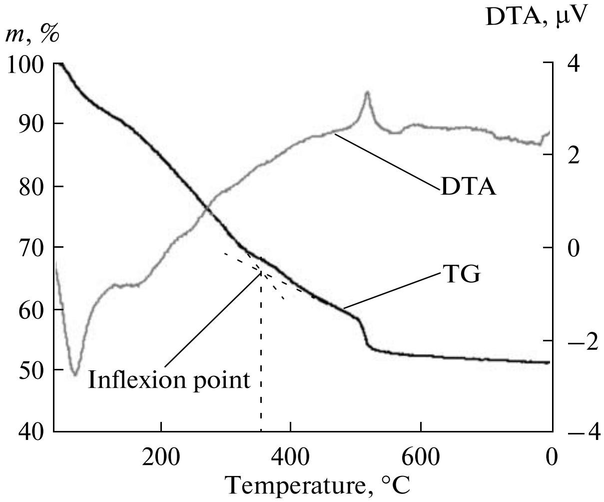

Fig. 2. TG-DTA curves for the precursor $MnCO_3$.

RESULTS AND DISCUSSION

Figure 1 shows the XRD pattern of the precursor. The sharp diffraction peaks of the pattern can be indexed to the 012, 104, 110, 113, 202, 024, 116, 122, 214 and 301 reflections of the rhodochrosite structure correspondingly according to the standard card JCPDS (44-1427). No characteristic peaks of other impurities were detected, indicating the high purity of the precursor. The crystallite size of the precursor estimated by the Scherrer formula is about 22 nm.

The thermal behavior of precursor $MnCO_3$ crystal was illustrated in Fig. 2. The TG curve shows a large weight loss range from the beginning to 520°C. The initial weight loss around 100°C is attributed to the loss of water which is corresponding to the first endothermic peak on the DTA curve. It can be seen from the TG curve that an indistinct inflexion point near 360°C can be discerned by the slope change of the TG curve as shown in Fig. 2. A phase transformation is considered to be possible around this inflexion point. The weight loss at 140–360°C is 24.77%.

Figure 3 shows the XRD patterns of the as-prepared samples calcined at different temperatures. As for the sample CT400 which was calcined at 400°C, the diffused broad peaks at 2θ = 37.12°, 42.24°, and 56.18° can be identified to the amorphous MnO_2 according to JCPDS (30-0820). While for CT600 and

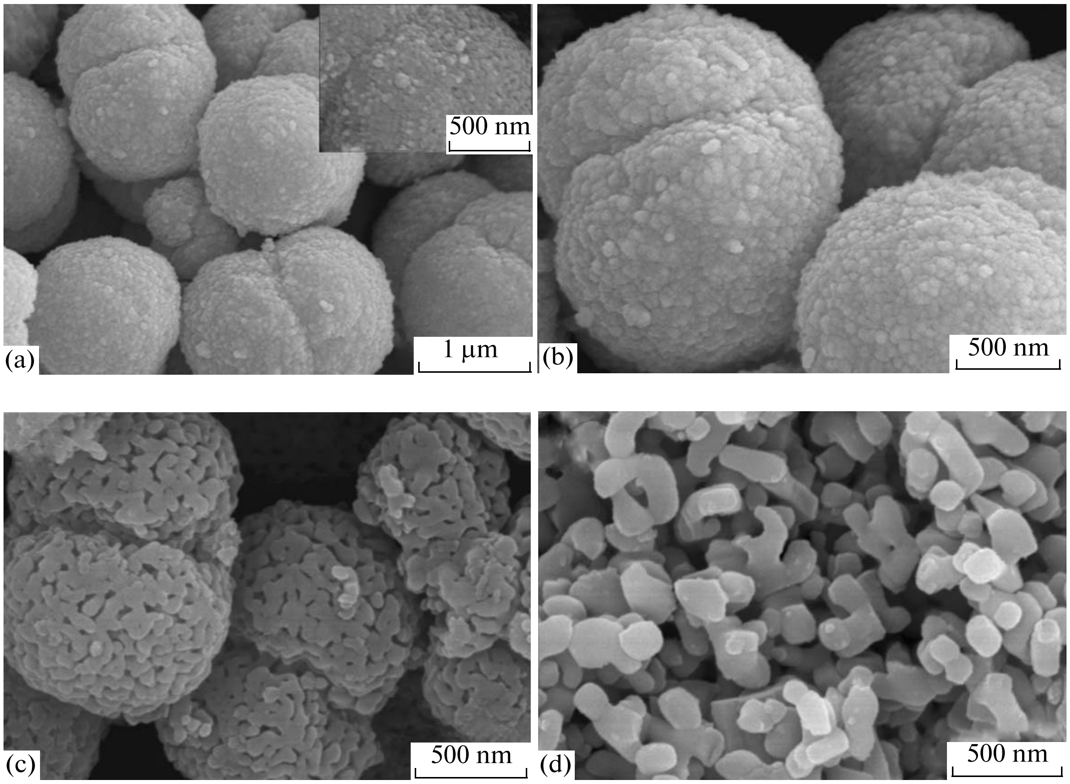

Fig. 4. SEM images of the precursor (a), sample CT400 (b), sample CT600 (c), sample CT800 (d).

CT800, the sharp diffraction peaks can be identified to be bixbyite (24-0508) as shown in Fig. 3 (scan *2* and *3*).

According to Biernacki's report [12], MnO was first formed accompanied with the emission of CO_2 during the first stage of the thermal decomposition of $MnCO_3$. Then MnO was prone to be oxidized by O_2 in the air simultaneously. The total reaction equation is shown as following:

$$2MnCO_3 + O_2 \longrightarrow 2MnO_2 + 2CO_2. \qquad (1)$$

The theoretical value of the solid weight loss during this process is 24.37%, which is very close to our detected result above. With the increase of temperature, it was considered that the irregular order of the amorphous phase recombined to form crystallized phase for receiving enough energy. The reaction is shown as following:

$$2MnO_2 \longrightarrow Mn_2O_3 + \frac{1}{2}O_2. \qquad (2)$$

This reaction is considered to happen above 500°C according to the TG curve, accompanied with a small exothermic peak close to 520°C on the DTA curve as shown in Fig. 2.

The morphology of the precursor as well as the calcined samples was detected by SEM measurement. The $MnCO_3$ crystal was spherical or nut-like which was aggregated by sub-crystalline of 20–30 nm as shown in Fig. 4a. The surface of the composite is coarse. After heating at 400°C, no obvious pore structure can be observed with the sample CT400 as shown in Fig. 4b. The surface morphology changed little compared with the precursor. It was interesting to observe macroporous structure (Fig. 4c) with sample CT600. The pore size and shape were irregular. With the heating temperature increasing up to 800°C, the pore structure collapsed to form flat lamella as shown in Fig. 4d.

Figure 5 shows representative nitrogen adsorption/desorption isotherms of sample CT400 and CT600. The isotherm of CT400 is type IV according to the classification of IUPAC. The hysteresis loop obtained from sample CT400 mainly present in the range of 0.4–0.9 P/P_0. Such adsorption behavior indicated the presence of the mesoporous structure. The specific surface area of this sample is 135.1 m^2/g as calculated by the Brunauer–Emmett–Teller (BET) formula. The sample CT600 exhibits an infrequent type III isotherm which indicates the presence of macroporous structure. The long hysteresis loop at $P/P_0 = 0.16–0.98$ indicates the broad pore size distribution. The specific surface area of sample CT600 is only 18.51 m^2/g, which may be caused by the vast transformation from mesoporous to macroporous.

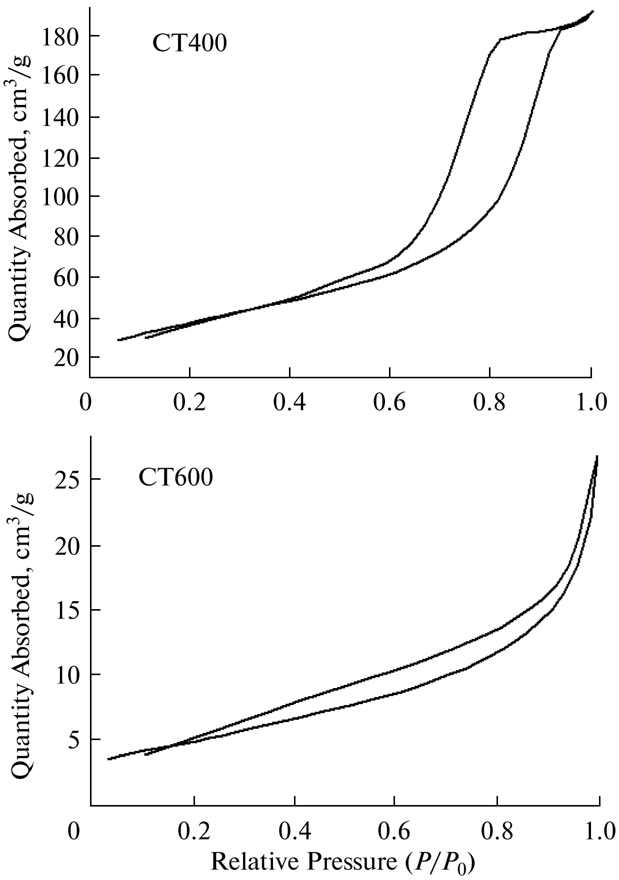

Fig. 5. N_2 adsorption-desorption isotherms for samples CT400 and CT600.

CONCLUSIONS

Porous manganese oxides are facilely prepared by a template-free thermal decomposition method. Micron-size $MnCO_3$ crystal was first prepared by a simple precipitation reaction. Porous manganese oxides were then obtained by the controlled thermal decomposition of the precursor $MnCO_3$. Amorphous mesoporous MnO_2 was obtained at 400°C which remained the surface morphology of the precursor and had a specific surface area of 135.1 m^2/g. Highly crystallized macroporous Mn_2O_3 was prepared at 600°C which had a specific surface area of 18.51 $m^2 g^{-1}$. This approach commendably simplified the preparation of mesoporous MnO_2 and macroporous Mn_2O_3 with brief process and low cost. Such method is supposed to be applied to the preparation of other porous oxides.

REFERENCES

1. Tian, Z.R., Tong, W., Wang, J.Y., et al., Manganese Oxide Mesoporous Structures: Mixed-Valent Semiconducting Catalysts, *Science*, 1997, vol. 276, no. 5314, pp. 926–930.
2. Finocchio, E. and Busca, G., Characterization and Hydrocarbon Oxidation Activity of Coprecipitated Mixed Oxides Mn_3O_4/Al_2O_3, *Catal. Today*, 2001, vol. 70, nos. 1–3, pp. 213–225.
3. Chitrakar, R., Kanoh, H., Miyai, Y., et al., A New Type of Manganese Oxide ($MnO_2 \cdot 0.5H_2O$) Derived from $Li_{1.6}Mn_{1.6}O_4$ and Its Lithium Ion-Sieve Properties, *Chem. Mater.*, 2000, vol. 12, no. 10, pp. 3151–3157.
4. Jiao, F., Harrison, A., Hill, A.H., et al., Mesoporous Mn_2O_3 and Mn_3O_4 with Crystalline Walls, *Adv. Mater.*, 2007, vol. 19, no. 22, pp. 4063–4066.
5. Suresh Raj, A.M.E., Mallika, C., Sreedharan, O.M., et al., Manganese Oxide-Manganese Tungstate Composite Humidity Sensors, *Mater. Lett.*, 2002, vol. 53, nos. 4–5, pp. 316–320.
6. Jiang, J.H. and Kucernak, A., Electrochemical Supercapacitor Material Based on Manganese Oxide: Preparation and Characterization, *Electrochim. Acta*, 2002, vol. 47, no. 15, pp. 2381–2386.
7. Fuertes, A.B., A General and Low-Cost Synthetic Route to High-Surface Area Metal Oxides through a Silica Xerogel Template, *J. Phys. Chem. Solids*, 2005, vol. 66, no. 5, pp. 741–747.
8. Xu, M.W., Zhao, D.D., Bao, S.J., et al., Mesoporous Amorphous MnO_2 as Electrode Material for Supercapacitor, *J. Solid State Electrochem.*, 2007, vol. 11, no. 8, pp. 1101–1107.
9. Zhu, S.M., Zhou, Z.Y., Zhang, D., et al., Synthesis of Mesoporous Amorphous MnO_2 from SB A-15 Via Surface Modification and Ultrasonic Waves, *Microporous Mesoporous Mater.*, 2006, vol. 95, pp. 257–264.
10. Yan, H.W., Blanford, C.F., Holland, B.T., et al., General Synthesis of Periodic Macroporous Solids by Templated Salt Precipitation and Chemical Conversion, *Chem. Mater.*, 2000, vol. 12, no. 4, pp. 1134–1141.
11. Jia, Z.G., Yue, L.H., Zheng, Y.F., et al., Crystallization Behavior and Thermal Decomposition of Characteristics Manganese(II) Oxalate in Organic-Water Binary Solvent System, *Chin. J. Inorg. Chem.*, 2007, vol. 23, no. 1, pp. 181–188.
12. Biernacki, L. and Pokrzywnicki, S., The Thermal Decomposition of Manganese Carbonate: Thermogravimetry and Exoemission of Electrons, *J. Therm. Anal. Calorim.*, 1999, vol. 55, no. 1, pp. 227–232.